

# Rescue of a severe mouse model for spinal muscular atrophy by U7 snRNA-mediated splicing modulation

Kathrin Meyer<sup>1,‡</sup>, Julien Marquis<sup>1,†,‡</sup>, Judith Trüb<sup>1</sup>, Rachel Nlend Nlend<sup>1</sup>, Sonia Verp<sup>2</sup>, Marc-David Ruepp<sup>1</sup>, Hans Imboden<sup>1</sup>, Isabelle Barde<sup>2</sup>, Didier Trono<sup>2</sup> and Daniel Schümperli<sup>1,\*</sup>

<sup>1</sup>Institute of Cell Biology, University of Bern, Baltzerstrasse 4, CH-3012 Bern, Switzerland and <sup>2</sup>Laboratory of Virology and Genetics, School of Life Sciences, EPFL Lausanne, Switzerland

Received October 9, 2008; Revised and Accepted November 10, 2008

**In spinal muscular atrophy (SMA), the leading genetic cause of early childhood death, the survival motor neuron 1 gene (*SMN1*) is deleted or inactivated. The nearly identical *SMN2* gene has a silent mutation that impairs the utilization of exon 7 and the production of functional protein. It has been hypothesized that therapies boosting *SMN2* exon 7 inclusion might prevent or cure SMA. Exon 7 inclusion can be stimulated in cell culture by oligonucleotides or intracellularly expressed RNAs, but evidence for an *in vivo* improvement of SMA symptoms is lacking. Here, we unambiguously confirm the above hypothesis by showing that a bifunctional U7 snRNA that stimulates exon 7 inclusion, when introduced by germline transgenesis, can efficiently complement the most severe mouse SMA model. These results are significant for the development of a somatic SMA therapy, but may also provide new means to study pathophysiological aspects of this devastating disease.**

## INTRODUCTION

The hypothesis that boosting the inclusion of exon 7 in the *SMN2* gene might provide an effective treatment or cure for SMA is based on the fact that all SMA patients have at least one, often several, *SMN2* copies (1,2). This copy number inversely correlates with the severity of the disease (3,4). However, there also appear to be modulating effects from other genes or of non-genetic origins (5–7).

Exon 7 of the *SMN2* gene is arguably one of the best studied exons of the human genome. It appears to be weak, as it is skipped, albeit infrequently, even in the functional *SMN1* gene. This weakness is due to a suboptimal intron 6 branch point (8), a non-canonical 5' splice site (ss), intronic splicing silencers (ISS) in both flanking introns and an inhibitory secondary structure towards the end of the exon (9). Positive elements are two exonic splicing enhancers (ESEs), termed SE1 and SE2, which contain binding sites for the splicing factors ASF/SF2 and hTra2 $\beta$ , respectively. In the *SMN2* gene, a silent mutation appears to weaken SE1 (10,11) and

may cause the formation of an additional hnRNP A1-dependent silencing element (12,13).

A stimulation of exon 7 inclusion has been achieved in cell culture models with antisense oligonucleotides that target either of the two ISS, the inhibitory sequences towards the end of exon 7, or, alternatively, mask the intron 7 branch point and 3' ss of exon 8 (9,14,15). In one of these studies, oligonucleotides were also introduced into a SMA mouse model, and splicing correction could be detected in liver and kidney. However, the oligonucleotides did not reach the spinal cord, and hence no therapeutic benefit could be demonstrated (15). Moreover, an elevation of SMN protein could recently be demonstrated after intracerebral injection of an oligonucleotide (16). Two studies, published in 2003, were using bifunctional oligonucleotides targeting the part of exon 7 that differs between *SMN1* and *SMN2* and additionally containing either an ESE sequence (17) or a peptide composed of alternating serines and arginines mimicking a SR protein (18). We have recently adapted several of these oligonucleotide-based approaches to an U7 snRNA-derived *in vivo* expression

\*To whom correspondence should be addressed. Tel: +41 31 631 4675; Fax: +41 31 631 4616; Email: [daniel.schuemperli@izb.unibe.ch](mailto:daniel.schuemperli@izb.unibe.ch)

<sup>†</sup>Present address: Laboratory of Virology and Genetics, School of Life Sciences, EPFL Lausanne, Switzerland.

<sup>‡</sup>The authors wish it to be known that, in their opinion, the first two authors should be regarded as joint First Authors.

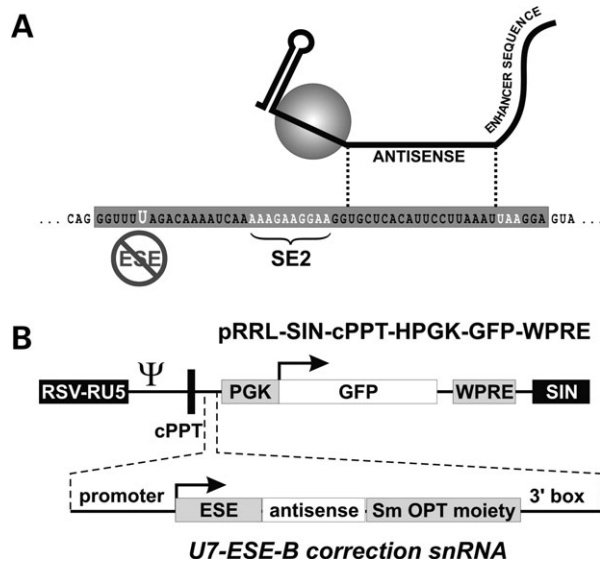


**Figure 1.** Structure of U7-ESE-B snRNA-containing LV used for mouse transgenesis. (A) The U7-ESE-B splicing correction cassette contains an antisense sequence directed to the 3' part of human *SMN2* gene exon 7 and an additional splicing enhancer sequence (19). The modified U7 moiety is represented by its 3' terminal stem loop and its Sm protein core (pictured as a grey ball). Within exon 7, the C to U transition that distinguishes *SMN1* and *SMN2* and that is thought to disrupt an ESE, the central ESE (SE2) and the UAA stop codon are indicated with white letters. (B) Structure of the LV pRRL-SIN-cPPT-hPGK-GFP-WPRE (32). The U7-ESE-B cassette is inserted upstream of the human phosphoglycerate kinase promoter in sense orientation with respect to the GFP open reading frame. Typical for a third generation vector, the 5' LTR contains U3 sequences from Rous sarcoma substituting for those of HIV-1 (RSV-RU5). The 3' LTR carries a self-inactivating (SIN) deletion. WPRE, woodchuck hepatitis virus post-transcriptional regulatory element; cPPT, HIV-1 central polypurine tract; Ψ, HIV-1 packaging signal.

cassette. Additionally, we have tried to improve exon 7 inclusion by using modified U1 and U2 snRNAs targeting the 5' ss and the intron 6 branch point, respectively (8,19). As a conclusion from these studies, we arrived at an optimal exon 7 inclusion strategy based on a bifunctional U7 construct (termed U7-ESE-B; Fig. 1A) which targets the 3' part of exon 7 and carries an ESE sequence that can attract stimulatory splicing factors (19). This construct induced a nearly complete exon 7 inclusion of a *SMN2-luciferase* reporter in HeLa cells as well as of the endogenous *SMN2* gene in SMA type I patient fibroblasts. In these fibroblasts, we also saw a 2- to 3-fold increase in SMN protein and, concomitantly, an increase of SMN-containing nuclear gems to a frequency also seen in certain wild-type cells or very mild forms of SMA (20). In the present study, we have introduced this U7-ESE-B cassette by transgenesis into the most severe SMA mouse model. We observe a clear suppression of disease-associated symptoms which can, in the most efficient cases, allow a normal weight development, muscle performance and life expectancy. These results fully confirm that exon 7 is the target of choice for SMA therapies, although future studies will have to show whether a correction starting after birth can still be beneficial. In addition, the transgenic approach in SMA mouse models should also be helpful for further investigations into SMA pathophysiology.

## RESULTS

### Therapeutic benefit of U7-ESE-B in a severe SMA model

We used the U7-ESE-B construct in a transgenic approach to test the hypothesis that the stimulation of *SMN2* exon 7 inclusion could alleviate SMA symptoms. U7-ESE-B transgenic mice were generated by lentiviral vector (LV)-mediated transgenesis (21). Two founder mice were chosen, based on cytofluorometric analyses of blood samples for the intensity of the green fluorescent protein (GFP) contained in the LV (Fig. 1B), and crossed with carriers of a mouse SMA model (described below). The mean fluorescence intensities and the numbers of integrated LV copies (determined by quantitative real-time polymerase chain reaction (PCR) of Gag and woodchuck hepatitis virus posttranscriptional regulatory element (WPRE) sequences) of these and further animals described below are documented in Supplementary Material, Table S1.

In the chosen SMA model, the most severe of its kind, the breeders are heterozygous for mouse *smn* (*smn*<sup>+/-</sup>) and homozygous for human *SMN2* (*hSMN2*<sup>+/+</sup>) and therefore have a similar genotype as human SMA carriers (22). The SMA-affected pups emerging from these breedings (*smn*<sup>-/-</sup>; *hSMN2*<sup>+/+</sup>) have an average lifespan of  $5.2 \pm 0.2$  days (23). In their terminal stage, they have the weight and appearance of 2–3-day-old normal pups.

When crossing the U7-ESE-B transgenic mice with SMA breeders, we found that both founder animals transmitted the GFP and U7 genes through the germline. GFP mean fluorescence intensities and integrated gene copy numbers decreased, on average, by a factor of 2 for each generation (Supplementary Material, Table S1), which suggested that the multiple integrations were not clustered. In successive crossings of the first generation offspring with SMA breeders, we obtained mice with the desired genotype: *smn*<sup>-/-</sup>; *hSMN2*<sup>+/+</sup>; U7-ESE-B<sup>+</sup> (variable copy numbers); these will henceforth be called SMA/U7 animals. For 15 of these SMA/U7 animals, a survival curve was established (Fig. 2). Copy numbers of the LV carrying the U7-ESE-B cassette varied between 1 and 12.5 in these animals (median 1.7). Six of these animals were censored (three for removal of tissues on day 32, one having died of an unrelated cause on day 275 and two mice remaining alive beyond 300 days). The other SMA/U7 animals died or were euthanized because of severe SMA symptoms between days 18 and 290. The median survival time was 123 days. In comparison, SMA mice (11 animals, seven censored because they were euthanized on days 3 or 4 based on genotyping) had a median survival time of 6.5 days. This is comparable with the average lifespan reported for such mice (23) (see above). Most importantly, the ~20-fold increase in survival times of SMA/U7 compared with U7 mice is highly significant ( $P < 0.0001$ ).

Two litters from U7-ESE-B bearing mothers with ~15 and ~seven LV copies per diploid genome which had eight and nine pups, respectively, were compared in more detail for their weight development during the first 2 months and for their muscle performance. Each of these litters consisted of three SMA/U7 pups, three *smn*<sup>+/+</sup> pups (termed wild-type) and two or three *smn*<sup>+/-</sup> pups (termed heterozygous), respectively (see Supplementary Material, Table S1 for more complete genotype description). Weights, general appearance,

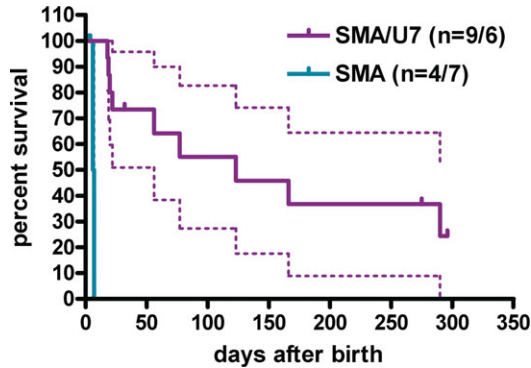


**Figure 2.** The presence of the U7-ESE-B cassette prolongs survival in SMA mice. SMA mice (turquoise) are homozygous for an insertional inactivation of the *smn* gene and homozygous for a human *SMN2* transgene (22). SMA/U7 mice (purple) additionally contain between one and 12 copies (median 1.7) of a LV carrying the U7-ESE-B cassette. Dashed lines indicate 95% confidence intervals. *n*, number of mice reaching endpoint (death or euthanasia due to severe SMA symptoms) or being censored, separated by a slash. Times when animals were censored are shown as upward blips. Reasons for censoring were: SMA, euthanasia after positive genotyping; SMA/U7, removal of tissues on day 32 (three animals), death of an unrelated cause (ear infection) on day 275 (one) and survival beyond the reporting period (two). The difference between the median survival times—123 days for SMA/U7, 6.5 for SMA—is highly significant ( $P < 0.0001$ ).

motility and additional disease-associated symptoms were initially recorded twice daily and later at wider intervals. Fig. 3 shows the weight development of these animals for the first 60 days after birth.

The three SMA/U7 pups (568, 573 and 575) born from mother 523 with the higher U7-ESE-B copy number had a nearly normal weight development, compared with their littermates (Fig. 3A). They contained between five and 12 LV insertions in their genomes (Supplementary Material, Table S1; Fig. 3C). They never showed any SMA-related disease symptoms (one of them died of an ear infection on day 275). One of these female SMA/U7 animals, 575, was bred with a wild-type male to see if it was able to carry, deliver and feed pups normally. Out of this coupling, seven pups were born which all developed normally beyond the time of weaning. These findings clearly show that the U7-ESE-B cassette can improve and sometimes even fully suppress the severe SMA symptoms.

In the litter of mother 558 with the lower U7-ESE-B copy number, two SMA/U7 pups showed a growth retardation after days 3–5 and their weight began to decrease at days 13 and 17, respectively (Fig. 3B). Based on criteria established in agreement with the animal experimentation authorities, these mice were euthanized on days 18 and 20, respectively. The other SMA/U7 pup from the same litter (580) had a reduced weight development and performed very weakly in a grid holding test (see below). It also displayed necrosis of the tail and of two toes on each hind foot. However, the necrosis stopped after some time, and the skin healed at these sites (Supplementary Material, Fig. S1). Such symptoms have been described previously for milder SMA mouse models (24). Importantly, mouse 580 did not display severe general disease symptoms, was always moving and eating well, until it died on day 290, apparently of a sudden SMA progression.

Grid holding tests (see Materials and Methods) performed on days 35, 42 and 56 after birth indicated that the SMA/U7 animal

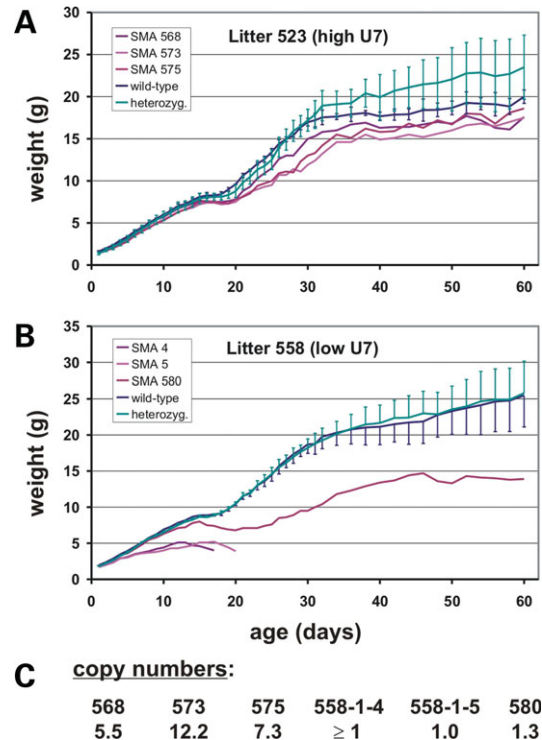


**Figure 3.** Weight development of SMA mice containing the U7-ESE-B cassette. Two female mice (*smn* ±; *hSMN2* ±; containing multiple copies of U7-ESE-B) were bred with SMA carrier males and the weight of their pups was measured at frequent intervals. (A) Mouse 523 (~30 copies of U7-ESE-B per diploid genome) had three SMA/U7 pups with two *hSMN2* copies, three wild-type and two heterozygous pups. (B) Mouse 558 (~seven copies of U7-ESE-B) had three SMA/U7 pups with two *hSMN2* copies, three wild-type and two heterozygous pups. The SMA/U7 pups 558-1-4 and 558-1-5 had to be euthanized on days 18 and 20, respectively. (C) Numbers of U7-ESE-B LV copies inserted in the genome of the above SMA/U7 mice. The real-time PCR indicated 0.5 copies in mouse 558-1-4, but non-quantitative PCR indicated that it contained at least one transgene copy. Animal identification: three digit numbers represent ear tag numbers introduced at weaning age. Animals killed at an earlier age are identified by the ID of their mother, the litter and a numbering system for animals of the same litter, based on foot tattooing on the day of birth (for example, 558-1-4 is pup 4 from the first litter of mother 558).

580 displaying disease symptoms was able to hold suspended on the grid for 6–30 s in the first, for 1–4 s in the second and not at all in the third test series (Fig. 4A, column 7). The symptom-free SMA/U7 animals 573 and 575 showed a completely normal holding time (columns 3 and 4). Only animal 568 had a reduced holding time in all tests (column 2), but seemed to improve with each new series (not shown). Note that a reduced performance was also observed in all three series for one of the heterozygous animals (581, data not shown but included in the wt/hz values; column 1). Thus, a reduced holding time may sometimes reflect an unwillingness to collaborate rather than a muscle weakness. Importantly, when the data of the three SMA/U7 animals from this litter were pooled, the median corresponded to the maximal length of the measurements, 120 s (column 5).

The SMA/U7 animals 568, 573 and 575 and their wild-type and heterozygous littermates were subjected to Rotarod running tests on days 88 and 105–107 after birth (summarized in Fig. 4B). It is evident from the graph that the SMA/U7

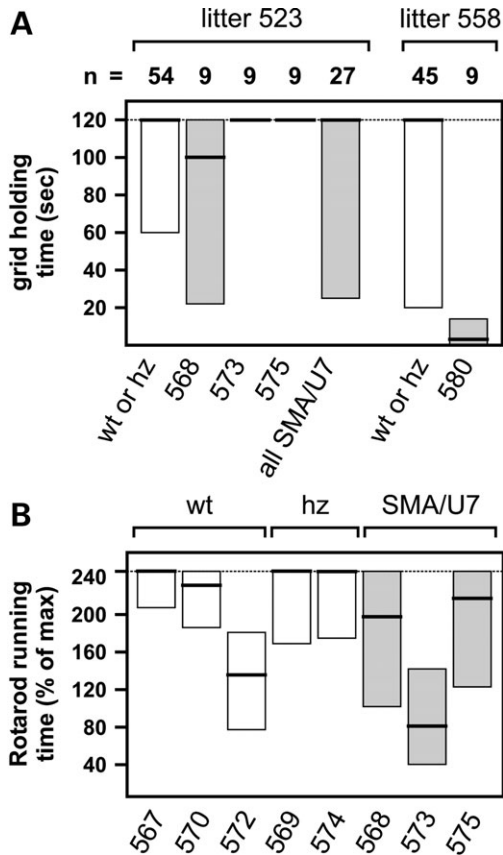


**Figure 4.** Muscle performance of SMA mice containing the U7-ESE-B cassette. **(A)** On days 35, 42 and 56, the ability of the remaining mice from litters 523-1 and 558-1 to hang suspended under a metal grid for up to 120 s was measured (three tests per day and mouse). *n*, number of individual test values. **(B)** On days 88 and 105–107, the mice from litter 523-1 were tested for their ability to run for up to 240 s on a Rotarod running device with the rotation speed increasing linearly from 10 to 40 rpm (six tests per day and mouse, 24 values in total). The boxes (grey for SMA/U7 mice, white for wild-type or heterozygous animals) encompass all values in the 10–90 percentile range. A thick horizontal bar indicates the median. Because of the maximum cut-off time, the values do not fall into a normal (Gaussian) distribution.

animal 573 performed considerably more weakly than the other two SMA/U7 animals and most of the wild-type or heterozygous mice from the same litter. However, the wild-type animal 572 also had a strongly reduced performance. The performances of the SMA/U7 animals 568 and 575 were only slightly reduced compared with those of the other wild-type or heterozygous littermates.

Taken together, these results demonstrate that a phenotypic improvement is observable in all SMA/U7 animals, but that it is variable, ranging from a short increase in life span to a virtually full suppression of all symptoms (e.g. in the SMA/U7 mouse 575).

#### Molecular and histological characterization of SMA/U7 mice

To determine how efficiently the U7-ESE-B snRNA corrects *hSMN2* splicing, we analysed total spinal cord RNA by reverse transcription (RT)-PCR. As the primers were not

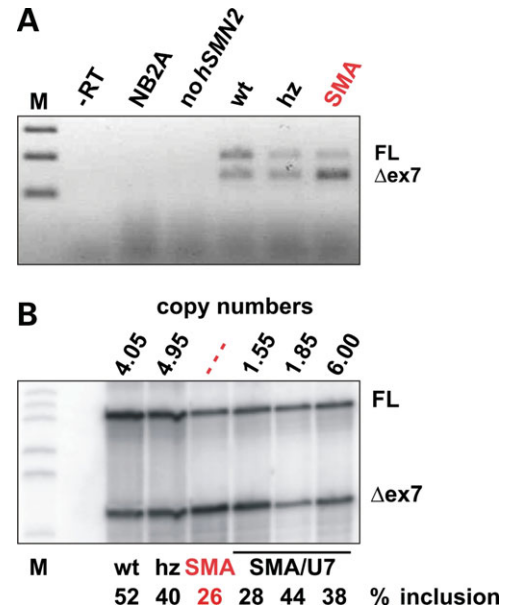


**Figure 5.** Increased *SMN2* exon 7 inclusion in SMA mice containing the U7-ESE-B cassette. **(A)** Gel with controls showing that the RT-PCR assay detects transcripts of human *SMN2*, but not mouse *smn*. NB2A, RNA from mouse neuroblastoma cell line NB2A; *no hSMN2*, RNA from spinal cord of a mouse that does not contain the human *SMN2* gene; the last three lanes correspond to the identically labelled lanes in (B); -RT, identical reaction as for the wt mouse, but with reverse transcriptase omitted; M, 100 bp size marker. The picture is a negative photograph of an ethidium bromide-stained agarose gel. The RT-PCR bands correspond to full-length *SMN2* mRNA (FL) and RNA lacking exon 7 ( $\Delta$ ex7). **(B)** RT-PCRs carried out with total spinal cord RNA from various mice. Note that all animals in the black labelled lanes (including wild-type [wt] and heterozygous [hz] ones) contain the U7-ESE-B cassette and hence show a splicing correction compared with the SMA mouse (red labelled lane). The numbers of integrated U7-ESE-B vector copies, as determined by quantitative PCR, are indicated above the lanes. The picture shows a denaturing polyacrylamide gel of reactions carried out in the presence of  $^{32}$ P-labelled dCTP. The per cent inclusion values were averaged from well correlating values of this gel scan and of a capillary electrophoretic analysis of an RT-PCR carried out with a fluorescently labelled downstream primer (see Materials and Methods). All samples were obtained at post-natal day 6, except for the SMA sample which was from a 3-day-old animal. M, size marker (end-labelled *HpaII* digest of pBR322).

complementary to mouse *smn*; RT-PCR bands were only obtained from mice containing the human *SMN2* gene, but not from *smn* +/+ mice lacking the human gene or from the mouse neuroblastoma cell line NB2A (Fig. 5A). To analyse the splicing correction, we used spinal cord RNA from 6-day-old wild-type, heterozygous and SMA mice with various numbers of integrated U7-ESE-B vector copies and from a 3-day-old SMA mouse lacking U7-ESE-B. As expected, in the spinal cord of the SMA mouse lacking a U7-ESE-B insert, only a small proportion of *hSMN2* mRNA contained exon 7 (26%; Fig. 5B). In contrast, all the mice containing the U7-ESE-B vector—wild-type, heterozygotes and SMA/U7—had an improved *hSMN2* exon 7 inclusion. Although there was no strict correlation, mice with higher U7-ESE-B copy numbers generally showed a stronger splicing correction. An improvement of exon 7 inclusion was also observed in RNA samples from other tissues (data not shown).

We then analysed the level of SMN protein in spinal cord extracts by western blotting (Fig. 6). All analysed animals

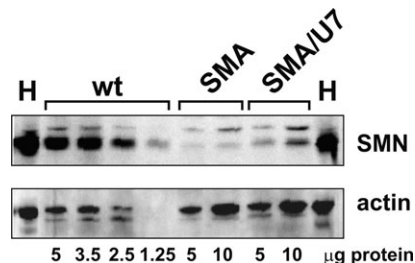


**Figure 6.** Increased SMN protein levels in SMA mice containing the U7-ESE-B cassette. Western blot detecting SMN and  $\beta$ -actin (loading control). The samples used were spinal cord lysates from 3-day-old animals 520-4-9 (wt; 2.5 U7-ESE-B copies; see Supplementary Material, Table S1), 608-2-1 (SMA) and 520-4-2 (SMA/U7; 5.3 U7-ESE-B copies). The amounts of protein loaded on the gel are indicated below the lanes. The anti-SMN antibody detects both human and mouse SMN. H, HeLa protein extract loaded as marker.

were 3 days old, and different amounts of extract were loaded on the gel to facilitate a semi-quantitative assessment. Accordingly, high levels of SMN were detected in wild-type (Fig. 6) and heterozygous animals (data not shown), which expressed mouse *smn* and *hSMN2* that was partly corrected. For the SMA mouse that expressed only uncorrected *hSMN2*, the intensity of the SMN band in 10  $\mu$ g of total protein was fainter than that seen in 1.25  $\mu$ g of wild-type extract. Thus it appears to contain less than one-tenth the amount of SMN in its spinal cord than a wild-type mouse. In contrast, the SMA/U7 mouse contained approximately one-fifth of the amount of SMN of the wild-type mouse but clearly more than the SMA animal without U7-ESE-B cassette. Similar results were obtained with other mice (data not shown). In conclusion, the presence of the U7-ESE-B allows for a clear but moderate increase in SMN protein level in the spinal cord.

To assess the preservation of motoneurons, 31-day-old animals from a single litter composed of three wild-type, heterozygous and SMA/U7 animals each were analysed. Spinal cord cross-sections sampled to reflect most of the body axis were stained with Toluidine blue (Fig. 7A). The number of large neuronal cells per ventral horn (considered to be motoneurons) showed a broad variation (data not shown). Since the sampling covered most of the length of the spinal cords and similar numbers of ventral horn sections (50–61) were counted in all animals, average values were used for comparison. This quantitative analysis revealed no significant difference between SMA/U7 animals and their wild-type and heterozygous littermates (Fig. 7B). We also isolated and stained spinal cords from 3-day-old SMA animals. However, although motoneurons were clearly visible (Fig. 7A), in our hands a reliable quantitative analysis was not possible due to the relatively poor tissue preservation and small size. It has been reported, though, that affected mice surviving up to day 5 show a loss of 35% of motor neurons in the spinal cord and 40% in the facial nucleus (22).

Although the western blot analysis had indicated a partial restoration of SMN protein expression in the spinal cord, it was important to know whether this was also true at the level of motoneurons. We therefore stained spinal cord sections from the same animals used for the histological analysis with anti-SMN antibody and used a 4',6-diamidino-

2-phenylindole (DAPI) counterstain to identify cell nuclei. Neuronal nuclei can be distinguished from those of other (mostly glial) cells based on their larger size and patchier DAPI staining (Fig. 7C). The cytoplasm of motoneurons from heterozygous (Fig. 7C, top row) and wild-type animals (not shown) gets intensely stained for SMN, but the nuclear space remains void of staining except for occasional gems. In the SMA animal (middle row), the cytoplasm of motoneurons showed virtually no staining. Staining of motoneurons was clearly recovered in spinal cord sections from SMA/U7 animals (bottom row), although it was weaker than in heterozygous or wild-type animals. The staining appeared to be somewhat more granular, but it is possible that a higher density of the same granules might suggest a more even distribution in the heterozygous or wild-type animals. Importantly, however, the staining also extended into axonal processes. Thus, these analyses show that SMN production is partly restored in SMA/U7 animals, not only at the total spinal cord level, but also within the motoneurons, the cells primarily affected in SMA.

## DISCUSSION

This study unambiguously and fully validates the hypothesis that SMA symptoms may be reduced or even completely suppressed by treatments that improve the utilization of *SMN2* exon 7. The range of phenotypic improvement seen in the SMA/U7 mice analysed here goes from short life prolongation or normal life span with pronounced SMA symptoms to full weight development, muscular function and the ability of a female to carry to term and feed a normal sized litter of pups.

Most of these animals contained one to seven copies of the U7-ESE-B transgene (except for one animal having 12 copies). There was no strict correlation between the number of integrated U7-ESE-B copies and the phenotype of the SMA/U7 pups, but animals with higher copy numbers tended to show fewer and less severe symptoms. Exon 7 inclusion in total spinal cord RNA was increased from 26 to 52%, and SMN protein levels were also increased, albeit only to an estimated one-fifth of the levels seen in wild-type or heterozygous animals. That such a small increase in SMN levels may have a significant impact on viability, and SMA symptoms are in agreement with the findings of Gavrulina *et al.* (25) who showed that low SMN cDNA expression in spinal cord can substantially prolong survival.

The fact that we saw only partial correction of *SMN2* splicing and low levels of SMN production could be traced to a very weak expression of the U7-ESE-B transgene that was hardly detectable by primer extension (Supplementary Material, Fig. S2). We have recently made the striking observation that different mouse U7 gene derivatives that we use for splicing correction are highly expressed in human, but poorly in mouse, cells (J.M. unpublished data). The reasons for this phenomenon are still under investigation, but this means that a higher expression might be expected in human patients, so that a single U7-ESE-B transgene per cell might be sufficient for a phenotypic correction. We are also investigating ways to improve the expression to achieve this goal.

These findings raise hopes for a therapy for SMA. As all patients carry at least one copy of *SMN2*, they may all

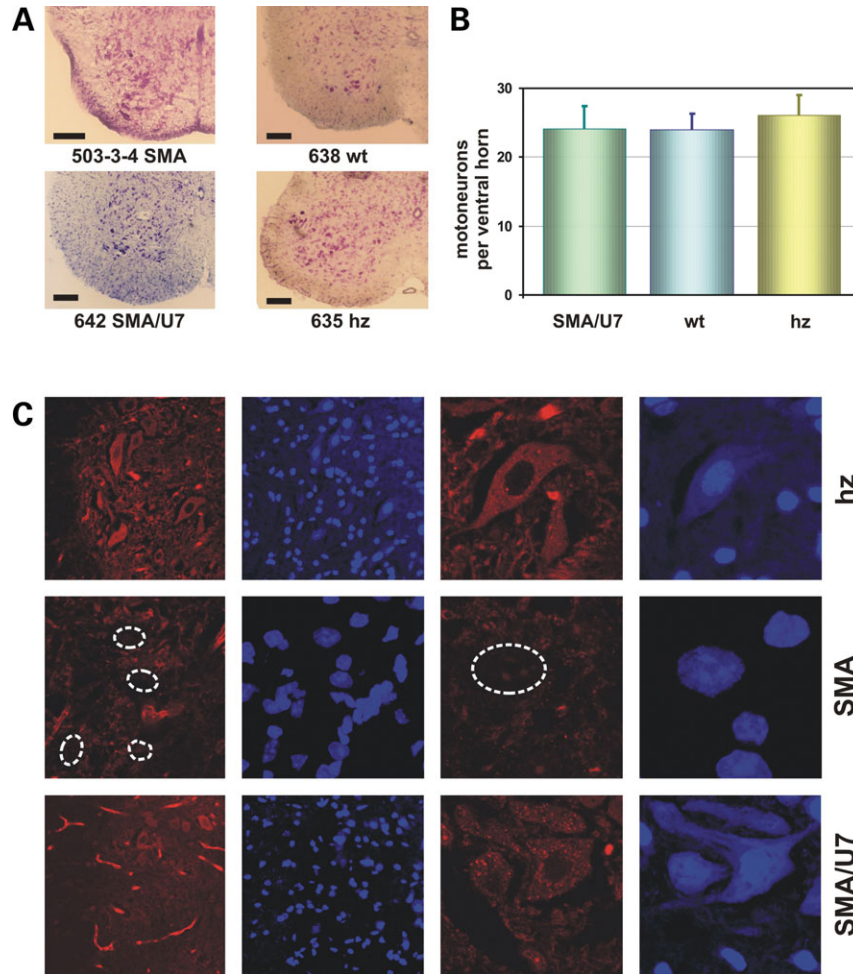


**Figure 7.** Preservation of motoneurons and SMN protein localization in SMA mice containing the U7-ESE-B cassette. (A) Toluidine blue staining of spinal cord cross-sections of the indicated mice. Mice 635 hz (heterozygote for *smn*), 638 wt (wild-type for *smn*) and 642 SMA/U7 were all from the same litter and 31 days of age; the SMA mouse 503-3-4 (from a separate litter) was 3 days old. (B) Counts of large neurons in spinal cord ventral horns of all nine animals (634–642) from the same litter. Five to seven sections from five different spinal cord areas separated about 5 mm from each other were used to count large neuronal cells in at least 50 ventral horns per animal. The average values from each animal were calculated, and the mean and standard deviation are shown for each group of animals (three animals per group). For the three SMA/U7 animals, the numbers of integrated U7-ESE-B vector copies as determined by quantitative PCR were between 1.2 and 1.9 (see Supplementary Material, Table S1). (C) Immunofluorescence analysis of SMN protein in spinal cord sections. The panels show overviews (left) and close-ups (right) with SMN immunofluorescence in red (single confocal planes) and DAPI staining of nuclei in blue (stack overlays). Samples shown are from heterozygous (hz) and SMA/U7 animals and from the 3-day-old SMA pup also used in (A). Staining patterns of wild-type animals were very similar to the ones shown for the heterozygous mouse. For the SMA animal, the areas occupied by some of the motoneuron nuclei are indicated by white interrupted lines to illustrate that the surrounding cytoplasmic area shows virtually no SMN staining. The red background staining comes from the secondary antibody which primarily binds to blood capillaries; in contrast no spill over was observed between the DAPI staining and the red channel.

benefit from a treatment able to improve exon 7 inclusion, particularly in motoneurons. However, there is still a long way to go, and it is presently unclear which type of therapy—small drugs, oligonucleotides or the type of therapeutic gene used here—will be first and most successful. Viewing its efficiency, our small U7-ESE-B gene is a good candidate, but its efficient and safe delivery to motoneurons will have to be established. Primary, but not exclusive, options are AAV vectors (26–28), but the serotype, strain and application routes must yet be elaborated.

Besides its importance in opening perspectives for SMA therapy, the transgenic approach that we have chosen also offers distinct possibilities to increase our knowledge about SMA in the mouse model. We have recently developed

a doxycycline-inducible system for the regulation of therapeutic U7 cassettes (29). We now plan to introduce this system into SMA mice by transgenesis in order to address important questions, such as when during ontogenesis low levels of SMN are particularly critical, whether there is a point of no return after which a therapy can no longer rescue the motoneurons from dying, or whether the disease will still develop if a correction of *SMN2* splicing is discontinued after the first phases of post-natal life. Additionally, mice can now be derived with stable single-copy insertions that should show intermediate SMA phenotypes due to partial *SMN2* splicing correction. These could be used to decipher molecular events occurring in the affected motoneurons, e.g. through the use of splicing microarrays. This is particularly important, because recent studies suggest

that the distribution of spliceosomal snRNPs and the splicing of many genes are deranged in a tissue-dependent manner, suggesting that SMA may be primarily a disease caused by splicing changes (30,31).

## MATERIALS AND METHODS

### Molecular cloning and LV transgenesis

The previously described U7-ESE-B splicing correction cassette (19) was amplified by PCR with the primers U7-5end-*Xho*I and U7-3end-*Eco*RV with *Pfu*-Ultra polymerase (Stratagene, La Jolla, CA, USA) according to the manufacturer's recommendations. For primer sequences see Supplementary Material, Table S2. The *Xho*I/*Eco*RV fragment was then transferred into the third generation LV pRRL-SIN-cPPT-hPGK-GFP-WPRE (32), between the cPPT and the hPGK promoter, in forward orientation with regard to eGFP. The entire U7 cassette and surrounding elements were verified by sequencing.

LVs were produced as described (33) except that supernatant was harvested twice (at 24 and 36 h post-transfection) and that serum-free Episerf medium (Gibco Invitrogen, Basel, Switzerland) was used instead of DMEM with fetal calf serum. LV transgenesis was carried out as described (21).

### Animal strains, breeding and husbandry

The SMA mouse strain (22) was obtained from Jackson Laboratory (strain name: FVB.Cg-Tg(SMN2)89Ahmb *smn1<sup>tm1Msd</sup>/J*, Stock number: 005024). These mice are heterozygous for a LacZ-Neo insertion in exon 2 of their *smn* gene and additionally carry two copies of the human *SMN2* transgene. Crosses between these animals result in progeny that are homozygous for the *smn* mutation and carry two copies of the *SMN2* transgene. Such animals have been reported to die between 4 and 7 days after birth (22,23). In contrast, homozygous *smn* knock-out mice without the *SMN2* transgene show embryonic lethality with an arrest in development before the stage of implantation (34).

The U7 transgene was inserted by LV-based transgenesis into oocytes of B6d2F2 mice (work performed in the laboratory of D. Trono at the EPFL, Lausanne, Switzerland) (21). Female transgenic animals were then crossed with SMA carrier males. A second cross with SMA carriers yielded mice of the desired genotype [*smn*<sup>-/-</sup>; *hSMN2*<sup>+/+</sup>; U7-ESE-B+ (multiple copies)], which are termed SMA/U7.

All mice were kept in individually ventilated cages in the animal facility of the Insel hospital in Berne, Switzerland in compliance with in compliance with legal requirements for animal husbandry and with the specific authorization issued for this project by the cantonal animal protection authority. In particular, litters with expected SMA genotypes were initially looked after twice daily and weighed once a day. Some older mice no longer used for experiments were moved to a conventional animal facility.

### Cytofluorometric GFP detection in blood samples

Approximately 50  $\mu$ l tail vein blood was mixed with 1 ml phosphate-buffered saline (PBS) containing 5  $\mu$ M EDTA and

centrifuged for 5 min at 500g and 4°C. The pellet was gently resuspended in 4 ml of red blood cell lysis buffer (150 mM NH<sub>4</sub>Cl, 10 mM KHCO<sub>3</sub> and 0.1 mM EDTA) and incubated for 10 min at room temperature in the dark. Cells were precipitated by centrifugation as above, and the red supernatant containing destroyed red blood cells was removed. Remaining cells were resuspended in 1 ml PBS, and GFP expression was measured by cytofluorometry (FACS Calibur, BD Bioscience, Meyrin, Switzerland). Age-matched blood not expressing GFP was used to define a negative population. The geometric mean of fluorescence intensity was determined with the FlowJo software version 7.2.4.

### Genotyping

Genomic DNA was isolated from tail biopsies, usually taken on the day of birth, by using the Wizard genomic DNA purification Kit (Promega AG, Wallisellen, Switzerland). For the PCRs, 20  $\mu$ l of reactants containing 50–200 ng genomic DNA, 400 nM of the corresponding primers (see Supplementary Material Table S2), 200  $\mu$ M of each deoxyribonucleotide triphosphate, 4  $\mu$ l of Q-solution and 1 U of *Taq* Polymerase (Qiagen AG, Hombrechtikon, Switzerland) were incubated for 30 s at 94°C, 1 min at 50°C and 2 min at 72°C for 40 cycles.

For the *smn* genotype, one common forward primer (mSmn Fw) and two reverse primers (mSmn Re and *Neo* border) were used. Intact and mutated *smn* yield products of 594 and 1200 bp, respectively. In heterozygous animals, both bands are produced. To determine the *SMN2* copy number, a common forward primer (Tg89-Grm7-Fw) was used, again together with two distinct reverse primers (Tg89-Grm7-Neg and Tg89-SMN-Re) (25). Thus, in heterozygous animals, two products of 280 and 372 bp were observed, representing the alleles with and without integration of *SMN2*, respectively. A qualitative assay for LV integration made use of the primer pWPTS-Sequencing and GFP10b and yielded an amplicon of 1406 bp in the positive case. For gender determination, the primers sry 3' and sry 5' yielded a male-specific product of 600 bp. For primer sequences see Supplementary Material, Table S2.

### Real-time PCR

Starting from 70 ng of mouse genomic DNA, we amplified Gag and WPRE sequences in the lentiviral construct, and Titin, a mouse housekeeping gene (35) (see Supplementary Material, Table S2 for primers and probes). The absolute amount of each gene was determined by referring to a standard curve. This consisted of a 10-fold serial dilution of a plasmid containing one copy of each of the genes, with known copy numbers at each dilution (six concentrations ranging from 10<sup>6</sup> to 10 copies for each gene). The absolute copy number of transgene integrated in the genome was obtained by dividing the amount of each reporter gene, Gag or WPRE, by half of the Titin amount, since the plasmid contains a single copy of the Titin gene, whereas the genomic DNA contains two copies. Values calculated with the Gag and WPRE assays correlated with a correlation coefficient  $R^2 = 0.9547$ , but WPRE-derived values were on average 20% higher. As it is not possible to say which assay is more correct, all values

presented in Supplementary Material, Table S1 and in the main manuscript are averages between the two determinations.

The real-time PCRs were run in simplex with the ABI Prism 7000 sodium dodecyl sulphate (SDS) v1.1 system (Applied Biosystem, Foster City, CA, USA). Mice genomic DNA or serial dilutions of the plasmid were included in a mix containing 2× Absolute QPCR Rox mix buffer (Thermo Scientific, Waltham, MA, USA), 162 nM of specific primers, 800 nM of corresponding TaqMan probe and water to a 18 µl final volume. The run conditions were as follow: 9600 emulation mode, one 15 min 95°C polymerase activation step, followed by 40 cycles of two-step qPCR (15 s of 95°C denaturation, 1 min of 60°C combined annealing/extension).

### Muscle performance tests

**Grid holding test.** Mice were placed on a grid and allowed to get a firm hold. Then the grid was turned upside down for 2 min, and the time for which the animals were able to hang on to the grid was measured. Three such tests were performed during each session, whereby the animals were allowed to recover for 1 min between the measurements. These tests were carried out three times with 1 week intervals.

**Rotarod assay.** This assay was carried out in the animal facility of the University of Fribourg, Switzerland with the kind support and advices from J. Schwaller and P. Gregory. After initial training sessions on a RotaRod device (TSE Systems GmbH, Bad Homburg, Germany), the mice were tested with a protocol applying accelerating speed of 10–40 rpm for up to 4 min. Each mouse did six trials per day, three in the morning and three in the afternoon; the break between the individual trials was at least 10 min, and the break between morning and afternoon was 3 h. The time that the animals were able to keep running was recorded. The data were analysed by using the Prism<sup>®</sup> software (GraphPad, San Diego, USA).

### RNA analysis

Total RNA was extracted with homemade Tri-Reagent (29) and resuspended in diethyl pyrocarbonate-treated water. Two micrograms of total RNA were reverse-transcribed into first-strand cDNA, by using 200 nM of oligo-dT, 50 U of Stratascript 6.0 reverse transcriptase (Stratagene), 1× Strata 6.0 buffer (Stratagene), 500 µM of all four dNTPs (Roche Diagnostics AG, Rotkreuz, Switzerland), 10 mM DTT and 8 U RNAsin (Promega) in a total volume of 50 µl.

PCRs including radioactive label were carried out with *Taq* DNA polymerase (Qiagen) in a volume of 25 µl with 5 µl of cDNA, 200 nM each of the SMN-Ex6-Fw (200 nM) and SMN-Ex8-Re primers, a mix containing 200 µM of dATP, dTTP and dGTP and 20 µM dCTP, 5 µCi  $\alpha$ -<sup>32</sup>P-dCTP (Hartmann Analytic GmbH, Braunschweig, Germany). Cycling conditions were 45 s at 95°C, 1 min at 50°C and 1 min at 72°C for 27 cycles. The PCR products were separated by electrophoresis on a 6% denaturing polyacrylamide gel. After exposure to phosphor storage screens (Molecular Dynamics, Sunnyvale, CA, USA), the intensity of radioactivity in the bands lacking (130 bp) or containing (184 bp) *SMN2* exon 7 was estimated with the AIDA software (version 2.31, Raytest Isotopenmessgeräte GmbH,

Straubenhardt, Germany) and values were corrected by normalizing them for the number of Cs in the molecule. In one experiment, the PCR was carried out in the absence of radioactive dCTP, but the forward primer was 5' end-labelled with 6-carboxyfluorescein (CF). The PCR product (1.2 µl) was mixed with 12 µl of GS500 LIZ standard (12.5 µl diluted in 1 ml of Hi-Di formamide, Applied Biosystems) and run for fragment analysis on an ABI 3100 sequencer (Applied Biosystems). The relative amounts of the products lacking or containing *SMN2* exon 7 were estimated from the areas of the corresponding peaks. The percentage of inclusion was calculated as the value of the included band divided by the sum of both products. The two methods yielded very similar results and the results were therefore averaged for inclusion in Fig. 5 of the paper.

For primer extension, 10 pmol of Pex-U7-Universal (detecting U7-ESE-B) or Pex-U2-WT (detecting endogenous U2 snRNA) primers were 5' labelled with 10 U of T4 polynucleotide kinase (New England Biolabs, Ipswich, MA, USA) in the presence of 20 pmol of  $\gamma$ -<sup>32</sup>P-ATP (Hartmann Analytic), and the labelled primers were used without further purification. Five micrograms of total RNA were slowly hybridized in a thermocycler with a mix of 100 fmol of both primers, and the RT reaction was performed as described above, except that the incubation was extended for 2 h. The products were separated on 15% denaturing polyacrylamide gels and the signals were analysed as described (19).

### Western blot

A polyclonal anti-SMN antibody was produced by immunizing New Zealand white rabbits with a recombinant protein corresponding to the first 180 amino acids of mouse SMN. Antibodies were affinity-purified with the recombinant protein used for immunization. Bound antibodies were eluted with 0.2 M glycine, pH 2.8, neutralized and stored at 4°C.

For western blots, tissue samples were lysed in RIPA buffer (137 mM NaCl, 10 mM phosphate, 2.7 mM KCl, 0.1% SDS, 0.5% sodium desoxycholate and 1% Igepal CA-630) supplemented with proteinase inhibitors (Complete EDTA-free, Roche). Extracts were resolved on 10% high-TEMED SDS-polyacrylamide gels and proteins were transferred onto reinforced nitrocellulose membranes (0.45 µm, Schleicher and Schuell, Bottmingen, Switzerland). SMN was detected with a 1:500 dilution of affinity-purified rabbit anti-mSMN antibody in TBS-tween-milk (Tris-buffered saline: 20 mM Tris-HCl, pH 7.5, 135 mM NaCl; supplied with 0.1% Tween 20 and 5% fat-free milk powder), while actin was detected by using a 1:500 dilution of the anti-actin (20–33) antibody (Sigma-Aldrich Chemie GmbH, Buchs SG, Switzerland) in TBS-tween-milk. The primary antibodies were then detected with a species-specific antibody coupled to horseradish peroxidase (Promega), and signals were visualized by the enhanced chemiluminescence method (Amersham Biosciences) and digitalized with the Luminescent Image Analyser LAS-1000 plus (Fujifilm AG, Dielsdorf, Switzerland).

### Histology and immunofluorescence

**Spinal cord sectioning, staining and neuron counting.** At post-natal day P31, spinal cords from the littermates 634–642 were



isolated and cut close to the cervical end. From there on, five pieces of 5 mm length were embedded in M-1 Embedding Matrix for frozen sectioning (six fluid OZ, Thermo Shandon, Pittsburgh) and kept frozen at  $-20^{\circ}\text{C}$  until use. From each 5 mm part, 10–12 cryosections of 25  $\mu\text{m}$  were cut with a Leitz 1720 Cryostat/Microtome (Leica Microsystems GmbH, Wetzlar, Germany), floating in PBS and then transferred to TBS containing 0.1% Triton X-100 from where they were taken onto microscope slides (superfrost, Menzel-Gläser, Braunschweig, Germany) and left to dry at least 5 h or over night. Then the slides were fixed in 100% ethanol for 10 min and transferred to the toluidine blue staining solution (1.2 g toluidine blue O and 3 g  $\text{Na}_2\text{CO}_3$  dissolved in 360 ml doubly distilled  $\text{H}_2\text{O}$ , 40 ml of 70% ethanol and 400 mg  $\text{NaN}_3$ ) for 6.5 min. Then, the slides were washed twice shortly in 70% ethanol and incubated for 1 min in 100% ethanol before putting them shortly in 100% xylol from where they were taken for embedding in Eukitt.

Before counting, the slides were blinded and assigned random numbers. All slides were then counted by a single person (that was not involved in the blinding) to minimize differences in counting criteria. A virtual line was drawn at the level of the central canal and all clearly visible large cells anterior to this line were considered to be neurons and counted. For each of the five regions of a spinal cord, at least 10 anterior horns were counted.

**Immunohistochemistry.** Cryosections from 31-day-old littermates 634 (WT), 635 (HZ) and 642 (SMA-U7), as well as from the 3-day-old mouse 504-4-4 (SMA, without therapeutic U7) were used. Floating sections were transferred from PBS into TBS. Then, the slides were incubated with TBS containing 1% Triton X-100 for 30 min and washed  $2 \times 10$  min with TBS followed by a 2-day incubation at  $4^{\circ}\text{C}$  with the monoclonal anti-SMN antibody 2B1 (Sigma, 1:500 diluted in TBS containing 1% BSA and 0.1%  $\text{NaN}_3$ ). Then, the sections were washed  $3 \times 10$  min in TBS before incubation with the secondary antibody goat-anti-mouse IgG conjugated to Alexa-594 (Invitrogen, 1:1000 diluted in TBS containing 1% BSA) for 2 h at room temperature in the dark. After washing  $3 \times 10$  min with TBS, the samples were incubated with DAPI (Invitrogen, 5  $\text{ng}/\mu\text{l}$  in TBS containing 1% BSA) and washed again  $3 \times 10$  min before they were transferred to microscope slides and embedded with Glycergel (Dako Inc., Carpinteria, CA, USA).

Preparations were analysed on an Eclipse 600 microscope equipped with a DXM1200 camera (Nikon, Tokyo, Japan) or on a Laser Scan Microscope SP2, (Leica Microsystems). Image processing was performed with ImageJ 1.34s (National Institutes of Health, Bethesda, MD, USA) and Corel Graphics Suite software (Corel GmbH, Unterschleissheim, Germany).

## SUPPLEMENTARY MATERIAL

Supplementary Material is available at *HMG* Online.

## ACKNOWLEDGEMENTS

The authors thank Karin Schranz and Alexandra Quazzola for technical help, Beat Schwaller and collaborators from the

University of Fribourg for instructions and permission to use their Rotarod device.

*Conflict of Interest statement.* None declared.

## FUNDING

This work was supported by AFM (Association Française contre les Myopathies), EURASNET (European Network of Excellence on Alternative Splicing), the Swiss Foundation for Research on Muscle Diseases and the Kanton Bern.

## REFERENCES

- Singh, N.N., Androphy, E.J. and Singh, R.N. (2004) The regulation and regulatory activities of alternative splicing of the SMN gene. *Crit. Rev. Eukaryot. Gene Expr.*, **14**, 271–285.
- Wirth, B., Brichta, L. and Hahnen, E. (2006) Spinal muscular atrophy: from gene to therapy. *Semin. Pediatr. Neurol.*, **13**, 121–131.
- Lefebvre, S., Burglen, L., Reboullet, S., Clermont, O., Burlet, P., Viollet, L., Benichou, B., Cruaud, C., Millasseau, P. and Zeviani, M. (1995) Identification and characterization of a spinal muscular atrophy-determining gene. *Cell*, **80**, 155–165.
- Feldkötter, M., Schwarzer, V., Wirth, R., Wienker, T.F. and Wirth, B. (2002) Quantitative analyses of SMN1 and SMN2 based on real-time lightCycler PCR: fast and highly reliable carrier testing and prediction of severity of spinal muscular atrophy. *Am. J. Hum. Genet.*, **70**, 358–368.
- Hahnen, E., Forkert, R., Marke, C., Rudnik-Schoneborn, S., Schonling, J., Zerres, K., Creavin, T. and Wirth, B. (1995) Molecular analysis of candidate genes on chromosome 5q13 in autosomal recessive spinal muscular atrophy: evidence of homozygous deletions of the SMN gene in unaffected individuals. *Hum. Mol. Genet.*, **4**, 1927–1933.
- Cobben, J.M., van der, S.G., Grootsholten, P., de Visser, M., Scheffer, H. and Buys, C.H. (1995) Deletions of the survival motor neuron gene in unaffected siblings of patients with spinal muscular atrophy. *Am. J. Hum. Genet.*, **57**, 805–808.
- Oprea, G.E., Krober, S., McWhorter, M.L., Rossoll, W., Muller, S., Krawczak, M., Bassell, G.J., Beattie, C.E. and Wirth, B. (2008) Plastin 3 is a protective modifier of autosomal recessive spinal muscular atrophy. *Science*, **320**, 524–527.
- Scholl, R., Marquis, J., Meyer, K. and Schümperli, D. (2007) Spinal muscular atrophy: position and functional importance of the branch site preceding SMN exon 7. *RNA Biol.*, **4**, 34–37.
- Singh, R.N. (2007) Evolving concepts on human SMN pre-mRNA splicing. *RNA Biol.*, **4**, 7–10.
- Cartegni, L. and Krainer, A.R. (2002) Disruption of an SF2/ASF-dependent exonic splicing enhancer in SMN2 causes spinal muscular atrophy in the absence of SMN1. *Nat. Genet.*, **30**, 377–384.
- Cartegni, L., Hastings, M.L., Calarco, J.A., de Stanchina, E. and Krainer, A.R. (2006) Determinants of exon 7 splicing in the spinal muscular atrophy genes, SMN1 and SMN2. *Am. J. Hum. Genet.*, **78**, 63–77.
- Kashima, T. and Manley, J.L. (2003) A negative element in SMN2 exon 7 inhibits splicing in spinal muscular atrophy. *Nat. Genet.*, **34**, 460–463.
- Kashima, T., Rao, N., David, C.J. and Manley, J.L. (2007) hnRNP A1 functions with specificity in repression of SMN2 exon 7 splicing. *Hum. Mol. Genet.*, **16**, 3149–3159.
- Lim, S.R. and Hertel, K.J. (2001) Modulation of survival motor neuron pre-mRNA splicing by inhibition of alternative 3' splice site pairing. *J. Biol. Chem.*, **276**, 45476–45483.
- Hua, Y., Vickers, T.A., Okunola, H.L., Bennett, C.F. and Krainer, A.R. (2008) Antisense masking of an hnRNP A1/A2 intronic splicing silencer corrects SMN2 splicing in transgenic mice. *Am. J. Hum. Genet.*, **82**, 834–848.
- Dickson, A., Osman, E. and Lorson, C. (2000) A negatively-acting bifunctional RNA increases survival motor neuron *in vitro* and *in vivo*. *Hum. Gene Ther.* doi:10.1089/hgt.2008.067.
- Skordis, L.A., Dunckley, M.G., Yue, B., Eperon, I.C. and Muntoni, F. (2003) Bifunctional antisense oligonucleotides provide a trans-acting

- splicing enhancer that stimulates SMN2 gene expression in patient fibroblasts. *Proc. Natl. Acad. Sci. USA*, **100**, 4114–4119.
18. Cartegni, L. and Krainer, A.R. (2003) Correction of disease-associated exon skipping by synthetic exon-specific activators. *Nat. Struct. Biol.*, **10**, 120–125.
  19. Marquis, J., Meyer, K., Angehrn, L., Kämpfer, S.S., Rothen-Rutishauser, B. and Schümperli, D. (2007) Spinal muscular atrophy: SMN2 pre-mRNA splicing corrected by a U7 snRNA derivative carrying a splicing enhancer sequence. *Mol. Ther.*, **15**, 1479–1486.
  20. Coovert, D.D., Le, T.T., McAndrew, P.E., Strasswimmer, J., Crawford, T.O., Mendell, J.R., Coulson, S.E., Androphy, E.J., Prior, T.W. and Burghes, A.H. (1997) The survival motor neuron protein in spinal muscular atrophy. *Hum. Mol. Genet.*, **6**, 1205–1214.
  21. Sauvain, M.O., Dorr, A.P., Stevenson, B., Quazzola, A., Naef, F., Wiznerowicz, M., Schutz, F., Jongeneel, V., Duboule, D., Spitz, F. and Trono, D. (2008) Genotypic features of lentivirus transgenic mice. *J. Virol.*, **82**, 7111–7119.
  22. Monani, U.R., Sendtner, M., Coovert, D.D., Parsons, D.W., Andreassi, C., Le, T.T., Jablonka, S., Schrank, B., Rossol, W., Prior, T.W. *et al.* (2000) The human centromeric survival motor neuron gene (SMN2) rescues embryonic lethality in *Smn*( $-/-$ ) mice and results in a mouse with spinal muscular atrophy. *Hum. Mol. Genet.*, **9**, 333–339.
  23. Le, T.T., Pham, L.T., Butchbach, M.E., Zhang, H.L., Monani, U.R., Coovert, D.D., Gavrilina, T.O., Xing, L., Bassell, G.J. and Burghes, A.H. (2005) SMN $\Delta$ 7, the major product of the centromeric survival motor neuron (SMN2) gene, extends survival in mice with spinal muscular atrophy and associates with full-length SMN. *Hum. Mol. Genet.*, **14**, 845–857.
  24. Tsai, L.K., Tsai, M.S., Lin, T.B., Hwu, W.L. and Li, H. (2006) Establishing a standardized therapeutic testing protocol for spinal muscular atrophy. *Neurobiol. Dis.*, **24**, 286–295.
  25. Gavrilina, T.O., McGovern, V.L., Workman, E., Crawford, T.O., Gogliotti, R.G., DiDonato, C.J., Monani, U.R., Morris, G.E. and Burghes, A.H.M. (2008) Neuronal SMN expression corrects spinal muscular atrophy in severe SMA mice while muscle-specific SMN expression has no phenotypic effect. *Hum. Mol. Genet.*, **17**, 1063–1075.
  26. Lu, Y.Y., Wang, L.J., Muramatsu, S., Ikeguchi, K., Fujimoto, K., Okada, T., Mizukami, H., Matsushita, T., Hanazono, Y., Kume, A. *et al.* (2003) Intramuscular injection of AAV-GDNF results in sustained expression of transgenic GDNF, and its delivery to spinal motoneurons by retrograde transport. *Neurosci. Res.*, **45**, 33–40.
  27. Foust, K.D., Poirier, A., Pacak, C.A., Mandel, R.J. and Flotte, T.R. (2008) Neonatal intraperitoneal or intravenous injections of recombinant adeno-associated virus type 8 transduce dorsal root ganglia and lower motor neurons. *Hum. Gene Ther.*, **19**, 61–70.
  28. Hollis, E.R., Kadoya, K., Hirsch, M., Samulski, R.J. and Tuszynski, M.H. (2008) Efficient retrograde neuronal transduction utilizing self-complementary AAV1. *Mol. Ther.*, **16**, 296–301.
  29. Marquis, J., Kämpfer, S.S., Angehrn, L. and Schümperli, D. (2008) Doxycycline-controlled splicing modulation by regulated antisense U7 snRNA expression cassettes. *Gene Ther.*, August 14 [Epub ahead of print] doi:10.1038/gt.2008.138.
  30. Gabanella, F., Butchbach, M.E.R., Saieva, L., Carissimi, C., Burghes, A.H.M. and Pellizzoni, L. (2007) Ribonucleoprotein assembly defects correlate with spinal muscular atrophy severity and preferentially affect a subset of spliceosomal snRNPs. *PLoS ONE*, **2**, e921.
  31. Zhang, Z., Lotti, F., Dittmar, K., Younis, I., Wan, L., Kasim, M. and Dreyfuss, G. (2008) SMN deficiency causes tissue-specific perturbations in the repertoire of snRNAs and widespread defects in splicing. *Cell*, **133**, 585–600.
  32. VandenDriessche, T., Thorrez, L., Naldini, L., Follenzi, A., Moons, L., Berneman, Z., Collen, D. and Chuah, M.K.L. (2002) Lentiviral vectors containing the human immunodeficiency virus type-1 central polypurine tract can efficiently transduce nondividing hepatocytes and antigen-presenting cells *in vivo*. *Blood*, **100**, 813–822.
  33. Barde, I., Zanta-Boussif, M.A., Paisant, S., Leboeuf, M., Rameau, P., Delenda, C. and Danos, O. (2006) Efficient control of gene expression in the hematopoietic system using a single Tet-on inducible lentiviral vector. *Mol. Ther.*, **13**, 382–390.
  34. Schrank, B., Gotz, R., Gunnarsen, J.M., Ure, J.M., Toyka, K.V., Smith, A.G. and Sendtner, M. (1997) Inactivation of the survival motor neuron gene, a candidate gene for human spinal muscular atrophy, leads to massive cell death in early mouse embryos. *Proc. Natl. Acad. Sci. USA*, **94**, 9920–9925.
  35. Charrier, S., Stockholm, D., Seye, K., Opolon, P., Taveau, M., Gross, D.A., Bucher-Laurent, S., Delenda, C., Vainchenker, W., Danos, O. and Galy, A. (2005) A lentiviral vector encoding the human Wiskott–Aldrich syndrome protein corrects immune and cytoskeletal defects in WASP knockout mice. *Gene Ther.*, **12**, 597–606.